

Influence of conducting polymer on mechanical, thermal and shape memory properties of polyurethane/polythiophene blends and nanocomposites

Rabia Sattar^{1,2}, Ayesha Kausar², Muhammad Siddiq^{1*}

¹Department of Chemistry, Quaid-i-Azam University, Islamabad 45320, Pakistan

²Nanosciences and Catalysis Division, National Centre for Physics, Quaid-i-Azam University Campus, Islamabad 44000, Pakistan

*Corresponding author. Tel: (+92) 51-90642147; Fax: (+92) 51-90642241; E-mail: m_sidiq12@yahoo.com

Received: 02 October 2015, Revised: 15 November 2015 and Accepted: 15 January 2016

ABSTRACT

Polyurethane/polythiophene (PU/PTh) blends and nanocomposites were prepared by solution mixing and in situ polymerization, respectively and were investigated for mechanical, thermal, electrical and shape memory properties. Formation of blends and composites was supported by FTIR analysis. Surface morphology of prepared samples was clarified by scanning electron microscopy (SEM). Homogeneous morphology of the composites was observed compared to blends due to well dispersion of NH₂ functionalized MWCNTs attributed to introduction of urea linkages between the functionalized nanotubes and the NCO-terminated PU. Smooth morphology of the composites resulted for the significant improvement of the mechanical properties. Thermal stability of the blends and composites was found increased with PTh content. According to differential scanning calorimetry (DSC), an increase in glass transition, melting and crystallization temperature was observed for composites with PTh addition. Maximum shape recoverability (92 %) was exhibited by the PU/PTh composite with 1 wt. % PTh loading. Copyright © 2016 VBRI Press.

Keywords: Conducting polymer; nanocomposite; mechanical testing; thermal analysis; shape memory behavior.

Introduction

Recently, the world of conjugated polymers and oligomers has recognized as an important branch of materials science with numerous applications in electronics and photonics. The potential usage of conducting polymers include as plastic batteries, sensors, conductive surfaces, magnetic recording, and solar cells [1-3]. Among conducting polymers, polythiophene (PTh) and its several derivatives has been synthesized and extensively investigated in the last 15 years because of their captivating electronic, optical, and semiconducting properties, combined with ease in production and chemically stable [4, 5]. However, enhanced thermal and environmental stability along with improved mechanical properties are anticipated for novel advances in the applications of conducting polymers. In order to improve these properties, current technological interest concerns the studies related to the preparations of composites, blends, or copolymers of the polythiophene with insulating polymers [4, 6, 7]. The preparation of such blend/composites would be aimed to synthesize the interesting advance materials possess a combination of good mechanical and thermal properties of insulating polymers and high conductivity of the constituent conducting polymers.

Among insulating polymers, polyurethane (PU) is a polymer showing high strain recovery, high degree of control on the softening/retraction temperatures and good physical properties [8]. The versatility of the PU can be further boosted through blend/composite formation and may have uses as rollers in electrostatic imaging, EMI shielding gasket materials, cables and chemical/biological sensors [9-14]. Recently, Sari *et al.* synthesized polyurethane/polythiophene (PU-PT) conducting copolymers using PU as an insulating matrix by electrochemical method [4]. Their structures and properties were analyzed using SEM, FTIR, DSC and TGA and were found that PU/PT copolymer was better thermally stable than the PTs. The urethane-substituted polythiophene blends were also reported to display enhanced optical properties as well as outstanding EMI shielding properties [15]. On the background of the above survey, we became interested in preparing polyurethane based blends and composite of polythiophene for which information appeared to be very meager.

In our work, we aimed to combine polyurethane insulating matrix with polythiophene conducting polymer. PU/PTh blends and PU/PTh/NH₂-MWCNTs composites with different contents of PTh (wt. %) were synthesized using solution blending and in situ polymerization, respectively. Synthesis of polyether based shape memory

block PU was carried out using polyethylene oxide, poly(propylene glycol)-*block*-poly(ethylene glycol)-*block*-poly(propylene glycol) as soft segment polyols and 2, 4-toluene diisocyanate as hard segment. All the prepared blends and composites were characterized by using FTIR, SEM, tensile testing, TGA, DSC and shape memory measurements. The formulations of samples carried out in this study are listed in **Table 1**.

Table 1. Formulations for samples used in this study.

| | PT03 | PT05 | PT10 | PTM03 | PTM05 | PTM10 |
|---------------------------------|------|------|------|-------|-------|-------|
| PU (NCO/OH) | 1.07 | 1.07 | 1.07 | 1.07 | 1.07 | 1.07 |
| PTh (wt. %) | 0.3 | 0.5 | 1.0 | 0.3 | 0.5 | 1.0 |
| NH ₂ -MWCNTs (wt. %) | – | – | – | 3.0 | 3.0 | 3.0 |

Experimental

Chemicals

Polyethylene oxide (MW ~ 100,000) (PEO), poly(propylene glycol)-*block*-poly(ethylene glycol)-*block*-poly(propylene glycol) (MW ~ 2,000) (PPG-*b*-PEG-*b*-PPG), 2,4-toluene diisocyanate (TDI, 99 %) were used in polyurethane synthesis and purchased from Aldrich. All these were degassed at 80 °C before use. Thiophene (99 %), iron chloride (FeCl₃·6H₂O, ≥98 %), ammonium bicarbonate (NH₄HCO₃, ≥99 %) and hydrochloric acid (HCl, 37 %) were received from Aldrich and used as received. Multi-walled carbon nanotubes (MWCNTs, 97–98 %) were procured from sigma. Their diameter was about 10–20 nm and length of 20–100 μm. Tetrahydrofuran (THF, 99.5 %) and ethanol (C₂H₅OH, ≥99.5 %) were purchased from Merck.

Preparation of polythiophene

The polythiophene (PTh) was synthesized by chemical oxidative polymerization method. The synthesis procedure was as follows; each thiophene monomer (0.84 g) and oxidant FeCl₃·6H₂O (6.76 g) was separately dissolved in 250 mL of 0.1 M HCl solution by constant stirring for 15 min. The molar ratio [oxidant]/[monomer] was 2.5. The oxidant solution was added to the monomer solution via dropping funnel under stirred condition. The preliminary polymerization process was identified by the color change (brown) of the reaction mixture. This synthesis was allowed to proceed for 6 h with constant stirring in ice bath. The dark-brown precipitates of polythiophene were recrystallized using 10 % NaOH solution. The mixture was kept for 24 h unagitated and PTh precipitates were collected by filtration and washed several times using distilled water. The obtained product was dried in oven at 50 °C for 24 h and finely grinded for further use.

Synthesis of PU/PTh blends

The synthesis of PU/PTh blend was carried out using solution mixing. First, polyurethane block copolymer was synthesized from its monomers, PEO, PPG-*b*-PEG-*b*-PPG and 2, 4-TDI having NCO/OH = 1.07 at 60 °C for 3 h under nitrogen atmosphere using THF solvent. Afterwards, PTh (preparation mentioned in above section) dispersed in THF was added to PU solution and polymerization reaction was allowed to proceed further for 12 h at 40 °C under constant stirring. At the end PU/PTh blend film was cast

onto the glass Petri dish and dried completely at room temperature. Three PU/PTh blend films with the varying weight % of polythiophene (0.3, 0.5 and 1 %) were prepared by following the same approach. Thickness of dried PU/PTh blend films was measured as 1 ± 0.05 mm.

Purification and amine functionalization of MWCNTs

Prior to functionalization, MWCNTs were purified in order to remove the metal content and other carbonaceous impurities. Purification was done by first annealing pristine MWCNTs at temperature of 400 °C for 0.5 h in furnace and then followed by the acid treatment. After annealing nanotubes were treated with HCl and reflux for 3 h. Finally, MWCNTs were filtered and washed with distilled water in order to remove the excess of HCl and oven dried at 60 °C for 10 h. After purification carbon nanotubes were amine (NH₂—) functionalized adopting ball milling technology using ammonium bicarbonate (NH₄HCO₃) [16]. For this drive, necessary amounts of MWCNTs and NH₄HCO₃ were mixed in the ratio of 1:3 and sonicated in ethanol for 3 h. Then mixture was dried via magnetic stirrer and put into a sinless steel ball milling container at 250 rpm for 4 h. After ball milling, the mixture was vacuum dried at 100 °C for 24 h to remove the residual gases. Upon ball milling, NH₄HCO₃ decomposed to form ammonia (NH₃), carbon dioxide and water molecules. So, NH₃ arising from the decomposition can form the covalent bonds with the broken —C—C— bonds of MWCNTs while CO₂ and water molecules will remove during oven drying. The obtained NH₂ functionalized MWCNTs were used to prepare PU/PTh/NH₂-MWCNTs composites.

Synthesis of PU/PTh/NH₂-MWCNTs composites

The fabrication of PU/PTh/NH₂-MWCNTs composite was done by in situ polymerization method. For this purpose three weight fractions of PTh (0.3, 0.5 and 1 %) and 0.1 g of NH₂ functionalized MWCNTs were dispersed in 20 mL of THF solvent and sonicated for 1 h at room temperature. Then each concentration of PTh/NH₂-MWCNTs was added to PU solution and mixture was allowed to react for 12 h at 40 °C under constant stirring. Finally, PU/PTh/NH₂-MWCNTs composite film was obtained by casting this solution mixture a glass Petri dish and dried completely at room temperature. All dried composite films had thickness of 1 ± 0.05 mm. Schematic structure of interaction between modified MWCNTs filled PU/PTh composite is shown in **Scheme 1**.

Characterizations

Infrared (IR) spectra were recorded on the Nexus 870 FT-IR spectrometer in transmission mode. The range for scan was selected from 4000–450 cm⁻¹. The recorded spectra were analyzed for the structural determination of the prepared samples. Scanning Electron Microscopy (SEM) of fractured samples was accomplished using Hitachi S-4800 in order to observe the morphology of the prepared blends and composites. The samples were fractured under liquid nitrogen, and then the fractured surfaces were vacuum-coated with a thin gold layer before observation. Thermogravimetric Analysis (TGA) of prepared films was performed on NETZSCH STA 449 C

thermal analyzer to determine the thermal stability of PU/PTh blend and composite films. The test was carried out in the temperature range of 25 – 700 °C under Nitrogen atmosphere using 7-10 mg of the sample in Al₂O₃ crucible at the heating rate of 20°C/min. A differential scanning calorimeter (DSC), Perkin–Elmer Pyris 1 DSC (Boston, MA, USA) was used for the analysis of phase transition temperatures of synthesized samples under an argon flow of 20 mL/min. For this analysis 5-7 mg of samples at heating rate of 10°C/min in the temperature range from 50 to 100°C were used. Stress-strain behavior of samples was examined using a universal testing machine (Instron 4466) with a strain rate of 5 mm/min at 23 °C according to ASTM D638 standard method. For this purpose, sample specimens of dimension 40×10×1±0.05 mm³ and a crosshead speed of 20 mm/min was used during the test. The shape-memory effect of rectangular strips with dimension 35×10×1±0.05 mm³ was observed by heating samples at 60 °C, while monitoring the shape recovery (SR) by using a video camera. The shape recovery was calculated using following Eq. (1).

$$SR(\%) = \{(90 - \theta) / 90\} \times 100 \quad (1)$$

where, θ in degree symbolizes the angle between the tangential line at the midpoint of the sample and the line joining the midpoint and the end of the curved samples.

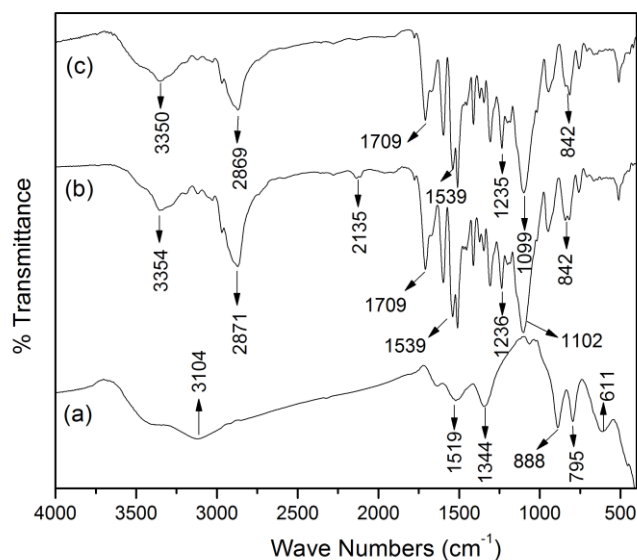


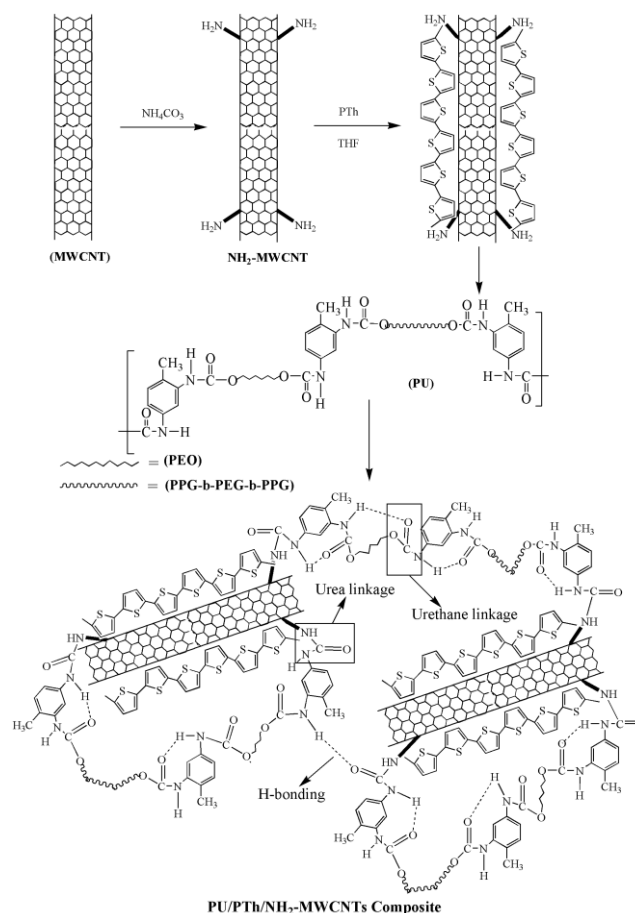
Fig. 1. FTIR spectra of (a) PTh; (b) PU/PTh blend; (c) PU/PTh/NH₂-MWCNTs composite.

Results and discussion

Spectroscopic analysis

The FTIR spectrum of PTh prepared from the chemical oxidative polymerization of thiophene is presented in the **Fig. 1(a)**. A band around 3104 cm⁻¹ is associated with C—H aromatic stretching vibration of PTh and adsorption of water molecules to PTh chains is responsible for the broadening of this band due to the accounting of OH stretching adjacent to C—H aromatic stretching vibration. The bands of weak intensities present at 2908 and

2848 cm⁻¹ correspond to the asymmetric and symmetric C—H stretching vibration, respectively. Absorption bands at 1519 and 1344 cm⁻¹ belong to the C=C asymmetric and symmetric stretching vibrations of thiophene ring, respectively. At 1063 cm⁻¹ the in-plane C—H aromatic bending vibrations of substituted thiophene ring is situated [17, 18]. A sharp band observed at 795 cm⁻¹ is attributed as 2, 5-substituted polythiophene associated with =C—H out-of-plane bending vibration mode [19]. The sharp band at 888 cm⁻¹ may be assigned to C—S stretching vibration. Another band appeared at 611 cm⁻¹ ascribed to the ring deformation of C—S—C in PTh [17].



Scheme 1. Reaction scheme for the preparation of PU/PTh/NH₂-MWCNTs composite.

Fig. 1(b) displays the FTIR spectrum of the PU/PTh blend. The wide band at 3354 cm⁻¹ is attributing the N—H stretching vibrations. The peaks at 1709 and 1670 cm⁻¹ assigned to free and hydrogen bonded carbonyl (C=O) stretching vibrations, respectively. The peak located at 1539 cm⁻¹ reflects the N—H bending vibration whereas a band at 1236 cm⁻¹ corresponds to the C—N stretching vibration mode. So, all above mentioned bands attributing to N—H, C=O and C—N vibrations verify the urethane linkages in the prepared PU/PTh blend. A strong band in the region of 1102 cm⁻¹ for C—O—C stretching vibration also provide strong evidence for the formation of urethane group. Besides this presence of peak at 842 cm⁻¹ due to the C—S vibration also confirms the presence of polythiophene structure in the PU matrix. The presence of —NCO band at

2135 cm^{-1} and very weak intense band of hydrogen bonded carbonyl stretching vibration suggest that PTh chains arranged themselves in between the PU chains and responsible for the reduction in inter chain hydrogen bonding in PU chains. FTIR spectrum of PU/PTh composite is presented in **Fig. 1(c)**. It is obvious from the spectrum that it shows resembles to the PU/PTh blend spectrum having characteristic urethane linkages peaks: N—H stretching vibration band at 3350 cm^{-1} ; free C=O stretching band at 1709 cm^{-1} ; H-bonded carbonyl stretching vibration band at 1671 cm^{-1} ; N—H bending band at 1539 cm^{-1} and C—N stretching vibration mode at 1235 cm^{-1} . The FTIR results indicate that band intensities of N—H and C—N stretching vibrations shifted towards the lower wave number in the composite suggest the formation of new urea linkages. The absence of isocyanate peak in composite spectrum also supported the presence urea linkages in the composite structure. These urea linkages are produced by the reaction of unreacted isocyanate groups with the —NH_2 groups of the amine functionalized CNTs (**Scheme 1**). The band assignments for Polythiophene, PU/PTh blend and composite spectra are listed in **ESI Table 1**.

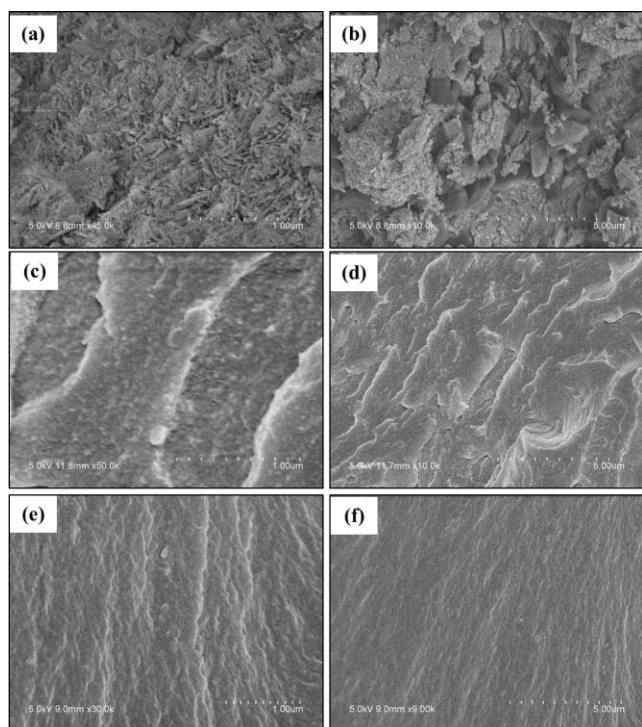


Fig. 2. FESEM images of (a) PTh at 1 μm ; (b) PTh at 5 μm ; (c) PT03 at 1 μm ; (d) PT03 at 5 μm ; (e) PTM03 at 1 μm ; (f) PTM03 at 5 μm .

Morphological investigation

The morphology of the synthesized PTh, its blends and nanocomposites containing 0.3 and 1 wt. % of conducting polymer with PU at different magnifications was recorded using SEM as shown in **Fig. 2 and 3**, respectively. The SEM images of PTh (**Fig. 2(a, b)**) showed a sponge-like and porous structure [5], but some fibrils are also present. The **Fig. 2(c, d)** shows the morphology of PU/PTh blend with the 0.3 wt. % PTh at two different resolutions. The surface morphology reflected a globular structure

representing presence of PTh chains in polyurethane matrix. Such a globular morphology resulted due to the lack of chemical interactions between PU and polythiophene chains. However, addition of amine functionalized MWCNTs in the nanocomposites produced smooth and homogeneous SEM images (**Fig. 2(d, e)**). Relatively fine micrographs of nanocomposites are attributed due to layered adsorption of PTh chains over the surface of nanotubes and well dispersion of MWCNTs in PU matrix as proposed in the reaction mechanism (**Scheme 1**). Presence of —NH_2 groups on the nanotube walls is responsible for their homogeneous dispersal in polymer matrix as these form the urea linkages by reacting with the —NCO groups of the isocyanate. **Fig. 3(a-d)** exhibits the morphology of PU/PTh blends and nanocomposites at higher loadings of PTh (1 wt. %) at different resolutions. Blend showed spherulitic structure also at higher content of polythiophene showing phase immiscibility (**Fig. 3(a, b)**). Comparatively, larger globules appeared in blend due to higher PTh content. The darker region formed the continuous phase associated to PU matrix and the dispersive spherical-like domains related to PTh phase. The composite images (**Fig. 3(c, d)**) showed homogeneously dispersion of nanotubes in polymer matrix. Presence of PTh chains onto the nanotubes surface and formation of urea linkages are responsible for the fine dispersal of MWCNTs leading to the phase compatibility for nanocomposites.

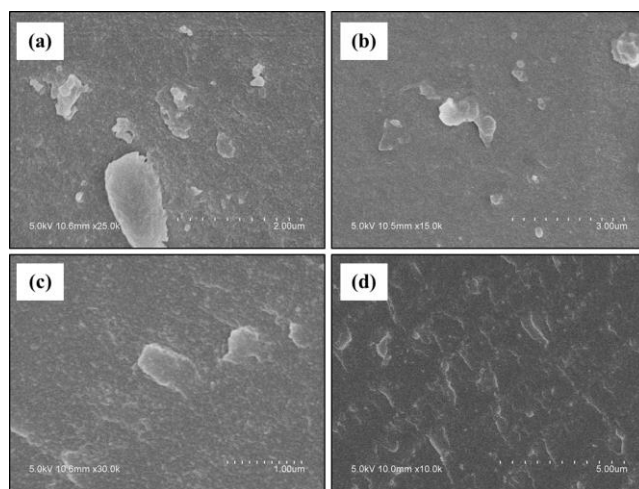


Fig. 3. FESEM images of (a) PT10 at 2 μm ; (b) PT10 at 3 μm ; (c) PTM10 at 1 μm ; (d) PTM10 at 5 μm .

Table 2. Mechanical properties and shape recovery of PU/PTh blend and PU/PTh/ NH_2 -MWCNTs composite films.

| | Ultimate Tensile Strength (MPa) | Elongation at Break (%) | Young's Modulus (MPa) | Shape Recovery (%) |
|-------|---------------------------------|-------------------------|-----------------------|--------------------|
| PT03 | 21.30 | 16.60 | 362.02 | 85 |
| PT05 | 20.68 | 15.70 | 341.51 | 83 |
| PT10 | 18.85 | 20.30 | 316.37 | 80 |
| PTM03 | 20.86 | 23.40 | 275.40 | 89 |
| PTM05 | 21.84 | 13.55 | 364.93 | 90 |
| PTM10 | 23.50 | 19.05 | 389.83 | 92 |

Mechanical properties

The mechanical properties for polyurethane blends and nanocomposites with varying wt. % of PTh are summarized in **Table 2**. It was noticed that for the blends, tensile strength and Young's modulus showed decreasing trend

with the rise of PTh content (**Fig. 4(a)**). Blend PT03 exhibited higher values of ultimate tensile strength and modulus 21.30 MPa and 362.02 MPa, respectively. This was attributing that higher content of conducting polymer (PTh) resulted in phase immiscibility (seen from morphology) as well as lowering of degree of hydrogen bonding in the hard segments of PU which responsible for the decline of mechanical properties. Ho and coworkers [20] also observed that tensile strength showed a monotonical drop for the PU/conducting polymer blend with lower degree of hydrogen bonding. On the contrary, elongation at break for blend films displayed an increasing trend with PTh content. This outcome was due to the presence of lower degree of hydrogen bonding in blends with higher loadings of PTh and caused to increase PU chains flexibility. **Fig. 4(b)** displays that for nanocomposite films, both Young's modulus and ultimate tensile strength increased with the rise of PTh content. The highest values of Young's modulus and ultimate tensile strength (389.83 MPa and 23.50 MPa, respectively) were observed for the functionalized MWCNTs and higher degree of hydrogen bonding owing to improved mechanical performance.

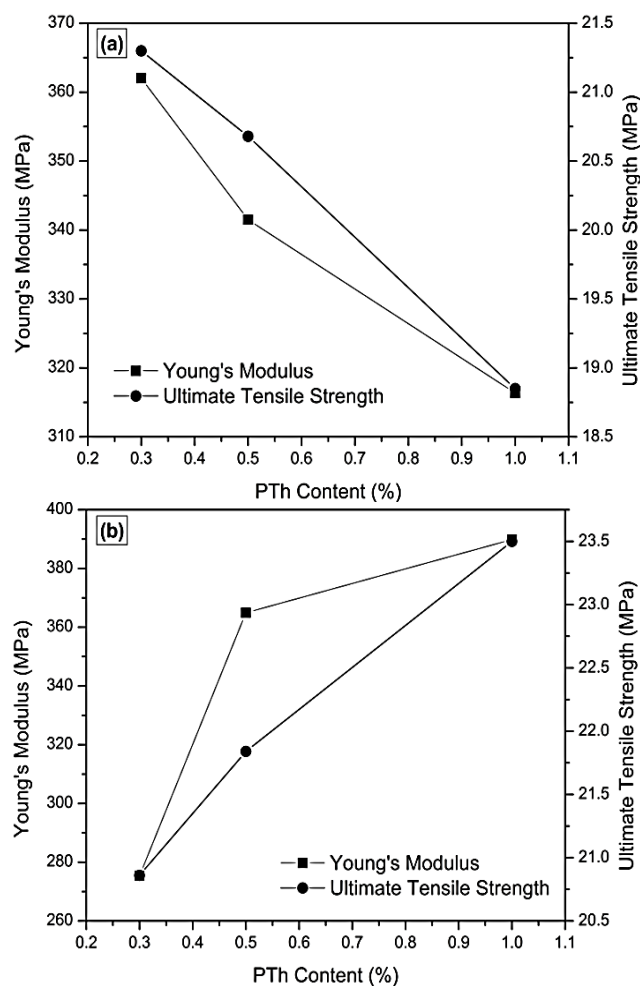


Fig. 4. Effect of PTh content on Young's modulus and ultimate tensile strength for (a) PU/PTh blend; (b) PU/PTh/NH₂-MWCNTs composite.

The interaction between N—H group present over the surface of nanotubes and —NCO from PU resulted to

produce urea linkages responsible for fine distribution of MWCNTs and phase mixing. Less interaction of PTh chains with PU are made due to the layered adsorption of PTh onto the nanotubes and resulted in the improved hydrogen bonding. So, these interactions (chemical and physical) in nanocomposites are the key factors for the enhanced mechanical properties. However, decrease in elongation at break was observed for nanocomposites with increase of PTh content. This was due to the presence of comparatively rigid structures of nanotubes and PTh chains in PU matrix.

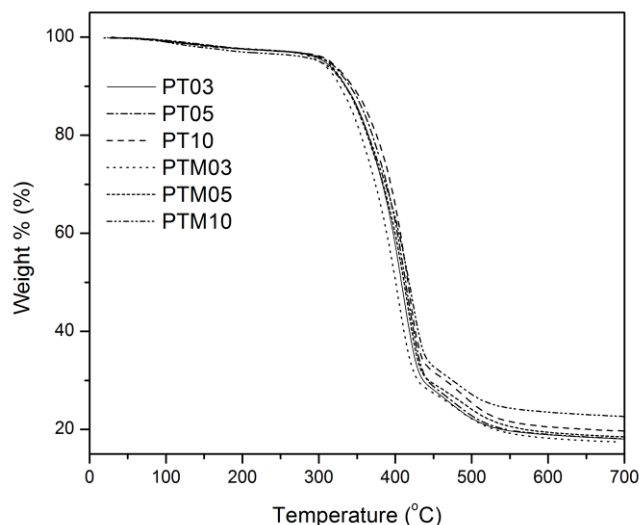


Fig. 5. TGA curves for PU/PTh blend and PU/PTh/NH₂-MWCNTs composite films.

Thermogravimetric analysis

The thermal behavior of PU/PTh blends and PU/PTh/NH₂-MWCNTs composites was studied using thermogravimetric analysis. The thermograms obtained for blends as well as nanocomposites are shown in **Fig. 5** and TGA decomposition data is listed in **ESI Table 2**. Decomposition of blends and nanocomposites was characterized by two degradation steps. The first degradation step was attributed to the degradation of hard-segment followed with the degradation of soft-segment of polyurethane comprising of polyols in second step [21]. It was noticed that the thermal stability of blends and nanocomposites increased with the increase in PTh content in PU matrix. The relative thermal stability of the prepared samples was compared by noting the on-set decomposition temperature (T_o), end-set decomposition temperature (T_e), and the char yield (Y_c). For the blend PT03, the initial weight loss for the first stage was observed starting at around 324 °C and the second one at about 435 °C. The addition of 1 wt. % PTh (PT10) resulted in the increase of initial degradation temperature of first and second one stage (6 °C and 3 °C respectively). The delay in degradation caused by the addition of PTh in blend films may be related to the presence of PTh chains in PU matrix and improvements of phase separation between soft and hard domains. PU/PTh/NH₂-MWCNTs composites showed the first stage of degradation in the temperature range of 320–325 °C and second stage of degradation in the range of 433–441 °C. It was also found that increase of PTh content

resulted in enhanced thermal stability of composite films. Notably, nanocomposites started to decompose at comparatively low temperature than blend films. This was most probably due to the surface adsorption of PTh chains on nanotubes and lack of chemical interactions between PU and polythiophene (**Scheme 1**). However, second degradation step for nanocomposites ensued at higher temperatures in comparison to blend films attributing the presence of thermally stable carbon nanotubes in composites. In addition, it was obvious that the higher char yield produced by the higher weight percent of PTh in the blends and nanocomposites due to the presence of improved thermally stable aromatic structure in the PTh chains. Maximum char residue (22.7 %) for the composite PTM10 resulted due to the higher content of PTh along with the nanotubes.

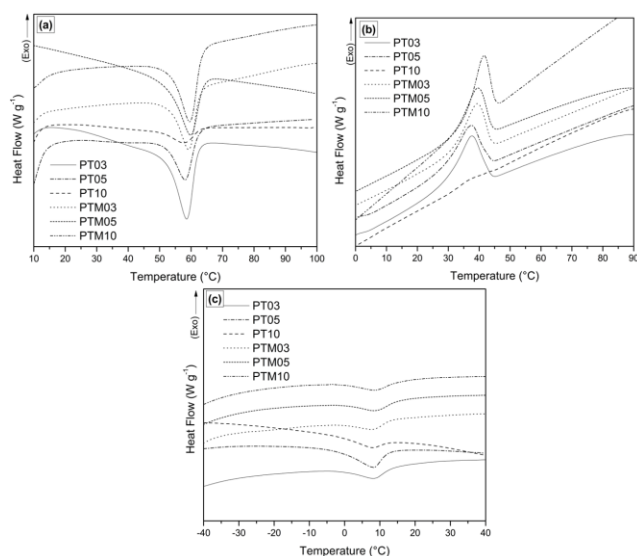


Fig. 6. DSC thermograms showing (a) melting temperature (T_m); (b) crystallization temperature (T_c); (c) glass transition temperature (T_g) for PU/PTh blend and PU/PTh/ NH_2 -MWCNTs composite films.

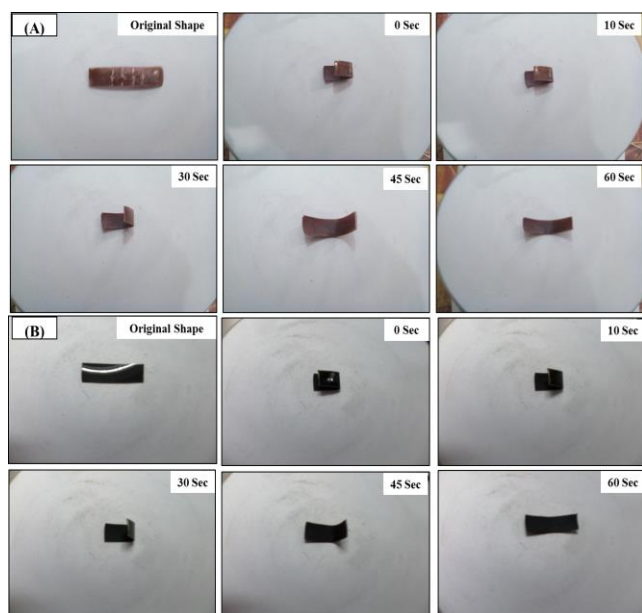


Fig. 7. Shape memory recovery of (A) PT10; (B) PTM10 heated at 60 °C.

Differential scanning calorimetry

DSC analysis of PU/PTh blends and nanocomposites are shown in **Fig. 6**. The heating (melting temperature (T_m)) and cooling (crystallization temperature (T_c)) DSC curves of prepared samples are displayed in **Fig. 6(a) and (b)**, respectively. Thermal transitions obtained from DSC study are listed in **ESI Table 3**. It was observed that crystallization and melting temperatures decreased with the increasing amount of PTh in blends, while in nanocomposites both T_m and T_c increased with PTh content. Melting temperature for the blend with 1 wt. % (PT10) appeared at 57.7 °C and only 2 °C rises in T_m was observed for the nanocomposite (PTM10). However, a significant shift was observed in crystallization behavior. As the addition of 1 wt. % PTh content for nanocomposite resulted in the rise of about 5 °C in crystallization temperature as compared to blend (PT10). This was attributed to layered adsorption of PTh chains onto the walls of MWCNTs and formation of urea linkages (between $-\text{NH}_2$ from nanotubes and $-\text{NCO}$ of PU). These both physical and chemical interactions between filler and matrix could be responsible for the rigidity of polymeric chains and enhanced the crystallization temperature. Beside this nucleating effect of nanotubes in composites is also evident from the increase in T_c and T_m [8, 22]. These findings also indicated that increase in chain rigidity and inclusion of amine functionalized MWCNTs were also responsible for an increase in glass transition temperature (T_g) for PU/PTh composites compared to blends as displayed in **Fig. 6(c)**. The well dispersion of the nanotubes as well as the formation of rigid structure through different molecular interactions (as stated earlier) is responsible for the increment of higher glass transition temperature.

Shape memory study

The shape memory property of the PU/PTh blends and PU/PTh/ NH_2 -MWCNTs composites is shown in **Fig. 7**. The composites exhibited well the shape memory property on addition of MWCNT as shown in **Table 2**. The shape memory behavior was observed by first bending the samples in U-shaped at transition temperature (T_{trans}), followed quenching to room temperature to obtain temporary shape and finally reheating it. The value of T_{trans} was taken 60 °C, closer to the T_m obtained from DSC studies. This belongs to T_m -type shape memory, because T_g is low and difficult to control the temperature around glass transition [23, 24]. When a surface temperature of 60 °C was given to the samples, shape changed spontaneously into that shown in **Fig. 7**. The original shape of the samples was nearly 80–92 % recovered approximately within 60 s. For PT03 85 % and PTM 03 89 % shape recovery was observed while maximum value of shape memory recovery of 92 % was appeared for PTM10. It was obvious that the incorporation of nanotubes directed to a noticeable enhancement in shape recovery. This fact can be attributed to the increased stored energy as a result of fine dispersed MWCNTs in the polymer matrix [25]. The nanotubes possessed higher stored elastic strain energy which assisted the composites to gain higher recovery stress due to release of stored elastic strain [26].

With the increase of PTh content in the nanocomposite, the shape recovery also found to be increased. It may be justified to associate the higher degree of crystallinity to this increasing trend of shape memory property. Consequently, a high degree of crystallinity (due to adsorption of PTh chains over the walls of MWCNTs) as well as both high electrical conductivity and mechanical properties may be required to show good shape recovery for composites.

Conclusion

PU/PTh blends and PU/PTh/NH₂-MWCNTs composites were synthesized by solution blending and in situ polymerization, respectively. The properties of the blends and composites were compared using FTIR, SEM, tensile, TGA, DSC and shape memory measurements. PU/PTh composite has smoother surface than PU/PTh blends due to the fine dispersion of nanotubes. The homogeneous morphology of the composites was accountable for the significant enhanced mechanical properties. The degradation temperature of the blends and nanocomposites was moved to higher values with the increase in PTh content. Loading of the modified nanotubes in the PU/PTh blend matrix also resulted in the improved glass transition, melting and crystallization temperature and these facts were corroborated to the both physical and chemical polymer-carbon nanotube interactions. Presences of the functionalized MWCNTs were also responsible for the significant improvement of the shape memory behavior of the resultant nanocomposites.

Acknowledgements

The authors acknowledge the financial support of Higher Education Commission, Islamabad, Pakistan under the indigenous PhD fellowship scheme (2PS1-487) and IRSIP program (IRSIP 24 PS 35).

Reference


- Wang, M.; Wang, X. *Sol. Energ. Mat. Sol. Cells* **2007**, *91*, 1782.
DOI: [10.1016/j.solmat.2007.06.006](https://doi.org/10.1016/j.solmat.2007.06.006)
- Pei, J.; Yu, W. L.; Huang, W.; Heeger, A. J. *Macromolecules* **2000**, *33*, 2462.
DOI: [10.1021/ma9914220](https://doi.org/10.1021/ma9914220)
- Takechi, K.; Shiga, T.; Motohiro, T.; Akiyama, T.; Yamada, S.; Nakayama, H.; Kohama, K. *Sol. Energ. Mat. Sol. Cells* **2006**, *90*, 1322.
DOI: [10.1016/j.solmat.2005.08.010](https://doi.org/10.1016/j.solmat.2005.08.010)
- Sari, B.; Talu, M.; Yildirim, F.; Balci, E. K. *Appl. Surf. Sci.*, **2003**, *205*, 27.
DOI: [10.1016/S0169-4332\(02\)01080-2](https://doi.org/10.1016/S0169-4332(02)01080-2)
- Özgün, A.; Sari, B.; Uygün, A.; Ünal, H. I.; Çakanyildirim, C. *Int. J. Polym. Anal. Charact.* **2009**, *14*, 469.
DOI: [10.1080/10236660903067474](https://doi.org/10.1080/10236660903067474)
- Sankir, M.; Kucukyavuz, S.; Kucukyavuz, Z. *Synth. Met.* **2002**, *128*, 247.
DOI: [10.1016/S0379-6779\(01\)00646-4](https://doi.org/10.1016/S0379-6779(01)00646-4)
- Ballav, N.; Biswas, M.; *Synth. Met.* **2004**, *142*, 309.
DOI: [10.1016/j.synthmet.2003.08.004](https://doi.org/10.1016/j.synthmet.2003.08.004)
- Sahoo, N.G.; Jung, Y. C.; Yoo, H. J.; Cho, J. W. *Compos. Sci. Technol.*, **2007**, *67*, 1920.
DOI: [10.1016/j.compscitech.2006.10.013](https://doi.org/10.1016/j.compscitech.2006.10.013)
- Isotalo, H.; Ahlskog, M.; Stubb, H.; *Synth. Met.* **1993**, *57*, 3581.
DOI: [10.1016/0379-6779\(93\)90480-K](https://doi.org/10.1016/0379-6779(93)90480-K)
- Wirpsza, Z.; *Poliuretany Chemia Technologia Zastosowanie*, Wydawnictwo Naukowo- Techniczne; Warsaw, **1991**, p.101.
DOI: [10.1016/0379-6779\(93\)90480-K](https://doi.org/10.1016/0379-6779(93)90480-K)
- Pelrine, R.; Kornbluh, R.; Joseph, J.; Heydt, R.; Pei, Q.; Chiba, S.; *Mater. Sci. Eng. C.*, **2000**, *11*, 89.
DOI: [10.1016/S0928-4931\(00\)00128-4](https://doi.org/10.1016/S0928-4931(00)00128-4)
- Koul, S.; Chandra, R.; Dhawan, S. K. *Sensor Actuat. B-Chem.*, **2001**, *75*, 151.
DOI: [10.1016/S0925-4005\(00\)00685-7](https://doi.org/10.1016/S0925-4005(00)00685-7)
- Gerard, M.; Chaubey, A.; Malhotra, B. D. *Biosens. Bioelectron.*, **2002**, *17*, 345.
DOI: [10.1016/S0956-5663\(01\)00312-8](https://doi.org/10.1016/S0956-5663(01)00312-8)
- Wang, Y. Z.; Hsu, Y. C.; Wu, R. R.; Kao, H. M. *Synth. Met.*, **2003**, *132*, 151.
DOI: [10.1016/S0379-6779\(02\)00207-2](https://doi.org/10.1016/S0379-6779(02)00207-2)
- Liu, M.; Gregory, R. V. *Synth. Met.*, **1995**, *72*, 45.
DOI: [10.1016/0379-6779\(94\)02317-R](https://doi.org/10.1016/0379-6779(94)02317-R)
- Ma, P. C.; Wang, S. Q.; Kim, J. K. *Carbon*, **2008**, *46*, 1497.
DOI: [10.1016/j.carbon.2008.06.048](https://doi.org/10.1016/j.carbon.2008.06.048)
- Gök, A.; Omastová, M.; Yavuz, A. G. *Synth. Met.*, **2007**, *157*, 23.
DOI: [10.1016/j.synthmet.2006.11.012](https://doi.org/10.1016/j.synthmet.2006.11.012)
- Gnanakan, S. P.; Rajasekhar, M.; Subramania, A. *Int. J. Electrochem. Sci.*, **2009**, *4*, 1289.
DOI: [electrochemsci.org/papers/vol4/4091289.pdf](https://doi.org/10.1016/j.electrochemsci.2009.04.012)
- Kelkar, D.; Chourasia, A. *Ch. & ChT*, **2011**, *5*, 309.
DOI: [ena.lp.edu.ua:8080/handle/ntb/11179](https://doi.org/10.1016/j.cht.2011.01.012)
- Ho, K. S.; Hsieh, K. H.; Huang, S. K.; Sieh, T. H. *Synth. Met.*, **1999**, *107*, 65.
DOI: [10.1016/S0379-6779\(99\)00144-7](https://doi.org/10.1016/S0379-6779(99)00144-7)
- Chattopadhyay, D. K.; Webster, D. C. *Prog. Polym. Sci.*, **2009**, *34*, 1068.
DOI: [10.1016/j.progpolymsci.2009.06.002](https://doi.org/10.1016/j.progpolymsci.2009.06.002)
- Manchado, M. L.; Valentini, L.; Biagiotti, J.; Kenny, J. M. *Carbon*, **2005**, *43*, 1499.
DOI: [10.1016/j.carbon.2005.01.031](https://doi.org/10.1016/j.carbon.2005.01.031)
- Hu, J.; Yang, Z.; Yeung, L.; Ji, F.; Liu, Y. *Polym. Int.*, **2005**, *54*, 854.
DOI: [10.1002/pi.1785](https://doi.org/10.1002/pi.1785)
- Yang, Z.; Hu, J.; Liu, Y.; Yeung, L. *Mater. Chem. Phys.*, **2006**, *98*, 368.
DOI: [10.1016/j.matchemphys.2005.09.065](https://doi.org/10.1016/j.matchemphys.2005.09.065)
- Rana, S.; Karak, N.; Cho, J. W.; Kim, Y. H. *Nanotechnology*, **2008**, *19*, 495707.
DOI: [10.1088/0957-4484/19/49/495707](https://doi.org/10.1088/0957-4484/19/49/495707)
- Ni, Q. Q.; Zhang, C. S.; Fu, Y.; Dai, G.; Kimura, T. *Compos. Struct.*, **2007**, *81*, 176.
DOI: [10.1016/j.compstruct.2006.08.017](https://doi.org/10.1016/j.compstruct.2006.08.017)

Advanced Materials Letters


Copyright © 2016 VBRI Press AB, Sweden
www.vbripress.com/aml

Publish your article in this journal

Advanced Materials Letters is an official international journal of International Association of Advanced Materials (IAAM, www.iaamonline.org) published monthly by VBRI Press AB from Sweden. The journal is intended to provide high-quality peer-review articles in the fascinating field of materials science and technology particularly in the area of structure, synthesis and processing, characterisation, advanced-state properties and applications of materials. All published articles are indexed in various databases and are available download for free. The manuscript management system is completely electronic and has fast and fair peer-review process. The journal includes review article, research article, notes, letter to editor and short communications.



A Monthly Journal



Supporting information

ESI Table 1. FTIR peaks assignment for PTh, PU/PTh blend and PU/PTh/NH₂-MWCNTs composite.

| Assignments | Wave number (cm ⁻¹) | | |
|--------------------------------------------|---------------------------------|------------|--------------------------------|
| | PTh | PU/PTh | PU/PTh/NH ₂ -MWCNTs |
| ν N—H | — | 3354 | 3350 |
| ν C—H (aromatic) | 3104 | 3028 | 3028 |
| ν_{as} C—H | 2908 | 2968 | 2968 |
| ν_{sym} C—H | 2848 | 2871 | 2869 |
| ν NCO | — | 2135 | — |
| ν C=O (Free) | — | 1709 | 1709 |
| ν C=O (H-bonded) | — | 1670 | 1671 |
| ν C=C—C (aromatic) | 1519, 1344 | 1597, 1509 | 1597, 1510 |
| δ N—H | — | 1539 | 1539 |
| δ_{as} C—H | — | 1454 | 1452 |
| δ CH ₂ & CH ₃ | — | 1412 | 1411 |
| δ_{sym} C—H | — | 1373, 1347 | 1373, 1346 |
| ν C—O | — | 1308 | 1307 |
| ν C—N | — | 1236 | 1235 |
| δ C—H (aromatic) | 1063 | 1199 | 1200 |
| ν C—O—C | — | 1102 | 1099 |
| ν C—C | — | 948 | 945 |
| ν C—S | 888 | 842 | 842 |
| subst Aromatic Ring | 795 | 817, 758 | 815, 757 |
| ω C—H (aromatic) | 795 | 707, 664 | 708, 664 |
| Ring deformation | 611 | 511 | 510 |

ν = stretch, δ = in-plane bending, ω = out-of-plane bending,
sym = symmetric, as = asymmetric, subst = substituted

ESI Table 2. TGA data of decomposition of PU/PTh blend and PU/PTh/NH₂-MWCNTs composite films.

| | First Step Degradation | | Second Step Degradation | | Y _c at 700°C (wt. %) |
|-------|------------------------|---------------------|-------------------------|---------------------|---------------------------------|
| | T _o (°C) | T _e (°C) | T _o (°C) | T _e (°C) | |
| PT03 | 323.9 | 435.5 | 435.5 | 548.9 | 18.1 |
| PT05 | 325.3 | 436.3 | 436.3 | 551.6 | 18.4 |
| PT10 | 330.8 | 438.5 | 438.5 | 553.1 | 19.1 |
| PTM03 | 319.9 | 433.2 | 433.2 | 550.2 | 17.5 |
| PTM05 | 322.6 | 437.2 | 437.2 | 551.6 | 18.5 |
| PTM10 | 325.3 | 441.2 | 441.2 | 552.9 | 22.7 |

T_o: On-set decomposition temperature, T_e: End-set decomposition temperature, Y_c: Char yield; weight of polymer remained

ESI Table 3. DSC data of decomposition of PU/PTh blend and PU/PTh/NH₂-MWCNTs composite films.

| | T _g (°C) | T _m (°C) | ΔH_m (J g ⁻¹) | T _c (°C) | ΔH_c (J g ⁻¹) |
|-------|---------------------|---------------------|-----------------------------------|---------------------|-----------------------------------|
| PT03 | 8.45 | 58.76 | 3.68 | 37.26 | 3.03 |
| PT05 | 8.25 | 58.11 | 2.84 | 37.09 | 2.67 |
| PT10 | 7.45 | 57.76 | 0.90 | 36.79 | 0.24 |
| PTM03 | 7.96 | 59.46 | 2.62 | 39.29 | 2.49 |
| PTM05 | 8.64 | 59.90 | 2.95 | 39.45 | 2.57 |
| PTM10 | 8.81 | 59.63 | 3.33 | 41.44 | 2.55 |

T_g: Glass transition temperature, T_m: Melting temperature, ΔH_m : Heat of melting, T_c: Crystallization temperature, ΔH_c : Heat of crystallization